Hapstick: A Soft Flexible Joystick for Stiffness Rendering via Fiber Jamming

Ayush Giri, Robert Bloom, and Tania K. Morimoto, *Senior Member, IEEE*

***Abstract*—Continuum robots are well-suited for applications in delicate and constrained environments, such as minimally invasive surgery, due to their inherent compliance and ability to conform to highly curved paths. Yet the kinematic dissimilarity between continuum robots and conventional, off-the-shelf input devices, along with the general lack of haptic feedback available with such devices, can lead to non-intuitive control. In this work, we present Hapstick — a soft, flexible haptic joystick that uses fiber jamming to modulate its stiffness and provide feedback to users during teleoperation tasks. We characterize the performance of Hapstick, showing that the bending stiffness increases linearly with the increase in applied vacuum load. A psychophysical study is also conducted to obtain the just noticeable difference in stiffness that users can perceive using Hapstick. Lastly, we perform a study in which participants use Hapstick to teleoperate a physical tendon-driven continuum robot in a simulated colorectal cancer screening task. Users correctly identify the position and development stages of cancerous tissues in 25 out of 27 trials, illustrating the potential of jamming-based mechanisms as bidirectional interfaces capable of providing effective haptic feedback.**

***Index Terms*—Haptics and haptic interfaces, medical robots and systems, telerobotics and teleoperation.**

I. Introduction

CONTINUUM robots are long, slender robots that can adjust their shape at any point along their length, similar to octopus tentacles and elephant trunks [1]. These robots offer many potential benefits for applications in highly sensitive and constrained environments, such as minimally invasive surgery, due to their inherent compliance and ability to navigate through curved paths [2]. These robots are typically controlled using a human-in-the-loop teleoperation scheme. However, the degree-of-freedom mismatch and kinematic dissimilarity between conventional input devices and continuum robots can result in less intuitive control [3] and introduce the need for complex mappings between the input devices and teleoperated robots [4]. In addition, many input devices lack the ability to provide users with haptic feedback, which can make certain tasks, such as tissue palpation, particularly difficult.

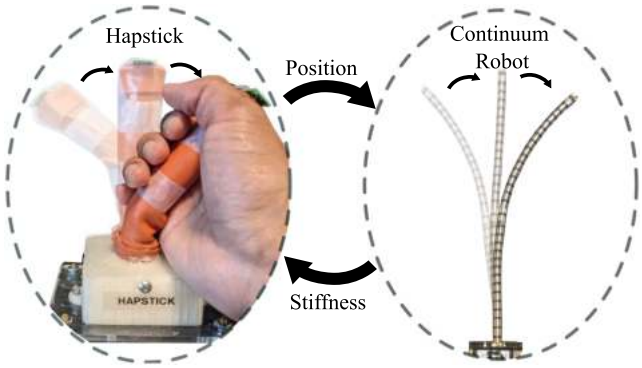

Fig. 1. Hapstick (left) is used to teleoperate a continuum robot (right). Hapstick acts as the leader device and its configuration, i.e curvature and angle of the plane containing the curvature, is directly mapped to that of the robot's distal segment. Hapstick can also display information about the stiffness of the robot's environment to the users by modulating its stiffness via fiber jamming.

To date, the most common approach has been to use commercially available input devices, including gamepads, 3D mice, and 6-DOF input devices (e.g. Geomagic Touch). However, recently, various input interfaces that are kinematically similar to continuum robots have started to be introduced as well. For instance, [5] presents a kinematically similar input leader device that allows intuitive shape control of multi-DOF continuum robots. Similarly, a flexible interface for teleoperating soft-growing robots is presented in [6]. The flexible device's design and structure offer "implicit" haptic feedback by rendering passive restoring spring forces to users. However, both [6] and [5] are unable to provide controllable haptic feedback, often critical for tasks such as tissue palpation and tissue identification. In [7], an impedance-type continuum input device that allows bidirectional teleoperation of continuum robots is presented. The device can provide force feedback via motors and cables to prevent users from commanding the robot to undesirable configurations. However, in order to provide feedback in multiple directions, the presented device requires a large, bulky setup with numerous motors, which increases the control complexity.

In this work, we present Hapstick (Fig. 1) — a soft, flexible haptic interface based on fiber jamming and designed to render stiffness information to users teleoperating a continuum robot.

Manuscript received 3 January 2023; accepted 7 May 2023. Date of publication 29 May 2023; date of current version 6 June 2023. This work was supported by the Arnold and Mabel Beckman Foundation. This letter was recommended for publication by Associate Editor K. B. Reed and Editor J.-H. Ryu upon evaluation of the reviewers' comments. *(Ayush Giri and Robert Bloom contributed equally to this work.) (Corresponding author: Ayush Giri.)*

This work involved human subjects or animals in its research. Approval of all ethical and experimental procedures and protocols was granted by the University of California, San Diego, Institutional Review Board.

Ayush Giri and Robert Bloom are with the Department of Mechanical and Aerospace Engineering and the Contextual Robotics Institute, University of California, San Diego, CA 92093 USA (e-mail: aygiri@eng.ucsd.edu; rl-bloom@ucsd.edu).

Tania K. Morimoto is with the Department of Mechanical and Aerospace Engineering, the Contextual Robotics Institute, and the Department of Surgery, University of California, San Diego, CA 92093 USA.

Digital Object Identifier 10.1109/LRA.2023.3280819

Jamming is a method of stiffening a system comprised of an external membrane and fillers, by collapsing the membrane onto the fillers, thereby increasing the density of the entire system [8]. To date, jamming-based interfaces have been shown to be lightweight, have low inertia, and provide passive stability [9]. Although various types of jamming materials have been proposed, in order for an input interface to be kinematically similar to continuum robots, it must be slender in structure. Granular jamming based slender structures cannot withstand large flexural loads [10], preventing them from acquiring configurations similar to flexible continuum robots. Similarly, layer jamming-based devices can only be bent in the direction perpendicular to the sheets, which limits such devices to allowing motion and generating forces in just a single direction [11]. Unlike granular jamming and layer jamming-based devices, fiber jamming-based interfaces can be bent in any direction and can also withstand large flexural loads [10]. While previous works ([10] and [12]) performed detailed analyses of fiber jamming technology, these studies mostly focused on material selection, modeling, and design optimization. The ability of fiber jamming-based devices to provide haptic feedback in the form of tunable stiffness has yet to be explored.

The contributions of this work are as follows. 1) Hapstick is the first fiber jamming-based input interface that can provide tunable stiffness feedback to the user. In addition to the ability to provide haptic feedback in any direction, the fiber jamming mechanism also allows Hapstick to have a kinematically similar structure to continuum robots, enabling potentially more intuitive control. 2) We present results showing the effect of the number of fibers on the ability of the device to provide uniform feedback to the users, as well as results characterizing the relationship between the applied vacuum load and the device stiffness. 3) We present a detailed user study performed to measure the just noticeable difference (JND) in the stiffness information that the users can perceive while using Hapstick. 4) We demonstrate Hapstick's applicability as a bidirectional interface with tunable stiffness for teleoperating a tendon-driven continuum robot in order to identify tumor positions and their development stages during colorectal cancer screening. Overall, Hapstick demonstrates the potential of jamming-based mechanisms as novel input interfaces that can provide effective haptic feedback to users.

II. System Design

In this section, we detail the working principles of Hapstick as a stiffness rendering device and as an input interface. We then present its design, fabrication, and overall workflow.

A. Working Principle

Hapstick is a fiber jamming-based device. Like other fiber jamming mechanisms, it consists of a soft tubular envelope that encloses flexible fibers that have a high coefficient of friction during mutual contact [10], [12]. When a vacuum load is applied inside Hapstick, its soft tube deforms inwards. The deformation compresses the fibers in the radial direction as shown in Fig. 2, resulting in an increase in the friction force between the fibers.

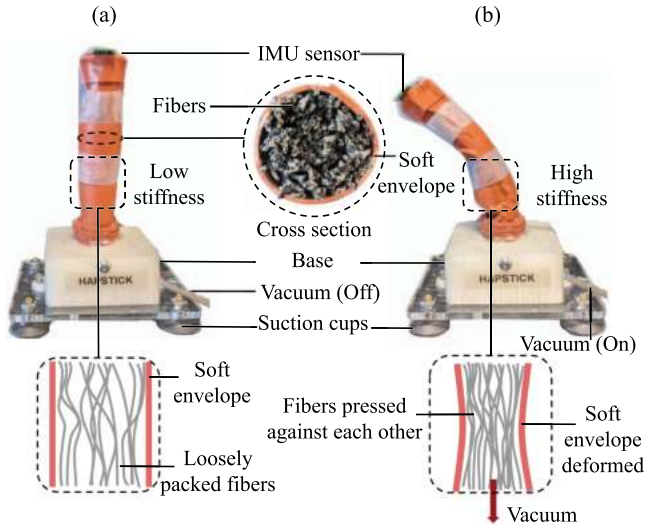

Fig. 2. Hapstick consists of a soft tubular envelope filled with flexible fibers and can be bent in any direction like a joystick. (a) When no vacuum load is applied, the fibers are loosely packed, and Hapstick is in a low stiffness state. (b) When a vacuum load is applied, the fibers are pressed tightly against each other, and the stiffness of Hapstick increases.

This increase in the friction force causes the fiber jamming-based structure to stiffen [10], and the resultant stiffness is dependent on the applied vacuum load. Users hold Hapstick with a power grip and as they bend it, they can feel the changes in Hapstick's stiffness as the vacuum levels are varied.

B. Design and Fabrication

Hapstick consists of a soft silicone sheet enveloping a set of abrasive, infill fibers. The silicone sheet is 0.80 mm thick and is first rolled into a tube with an outer diameter of 25 mm and a height of 110 mm. The outer diameter was selected to ensure it was within the range recommended for ergonomic cylindrical handles [13], and the height allows Hapstick to be comfortably bent into a single curve. A known number of abrasive fibers are then filled inside the silicone tube, running along the entire length. Mitchell abrasive fibers (aluminum oxide 180 grit, 0.76 mm diameter) are selected since they have previously been shown to provide a large flexural stiffness to slender structures when subjected to large vacuum loads [10]. The two open ends of the joystick are then sealed with circular silicone discs using a silicone adhesive (Smooth-on Sil-poxy). Hapstick's fabricated body is then inserted 10 mm into a 3D printed base that is rigidly attached to a rectangular acrylic sheet. The acrylic sheet has four suction cups, which help stabilize the setup. Finally, a tube is routed through the 3D-printed base and attached to the bottom of Hapstick to supply the fiber jamming-based device with a vacuum load. An IMU (Pololu MinIMU-9 v5) sensor is then mounted on top of the fabricated Hapstick and is used to map Hapstick's tip orientation to the teleoperated robot's configuration as detailed in the subsequent section. A Proportional Air (QBX Series) vacuum regulator, which is capable of regulating 0 kPa to -100 kPa, is used to provide the vacuum load to Hapstick. An Arduino Uno and a computer are used to

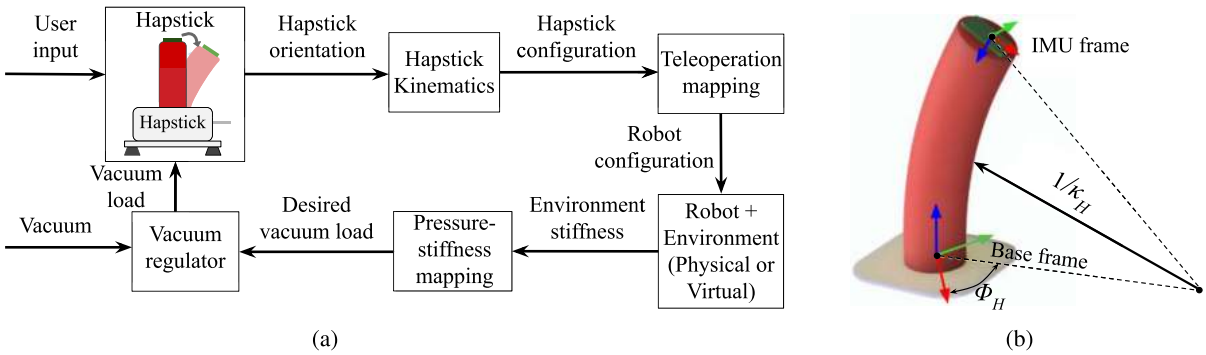

Fig. 3. (a) Schematic showing the workflow for teleoperating a robot and rendering stiffness feedback using Hapstick. (b) Schematic of Hapstick in a bent configuration with the geometric parameters, κ_H and ϕ_H, used in the employed mapping technique.

control both Hapstick's input and feedback capabilities. Fig. 2 shows a fabricated and assembled Hapstick in the unjammed and jammed states.

C. System Workflow

The overall system workflow is illustrated in Fig. 3(a). Without any vacuum load, Hapstick has a low bending stiffness. It can therefore be easily bent in any direction to mimic a segment of a continuum robot, physical or virtual. When a user bends Hapstick, Euler angles representing the tip orientation can be tracked using the IMU. Assuming constant curvature bending, the orientation information can be converted into the curvature (κ_H) and the angle of the plane containing the curvature (ϕ_H) [4], as shown in Fig. 3(b), in order to obtain its configuration.

Hapstick's configuration is then mapped to the desired configuration of a follower continuum robot as follows: $\kappa_R = \alpha\kappa_H$ and $\phi_R = \phi_H$, where κ_R is the distal segment of the continuum robot, α is a scaling factor selected to accommodate for length differences between Hapstick and the robot, and ϕ_R is the angle of the plane containing the robot's curvature. Alternative mappings for coupling Hapstick with other continuum robots, such as tip extending robots and concentric tube robots, can be explored.

Based on the interaction — physical or virtual — of the teleoperated robot with the environment, stiffness information can then be conveyed to the user via Hapstick. This stiffness information can be obtained using robots that are equipped with sensors capable of measuring stiffness [14], or by robots operating within virtual environments [15]. The vacuum load required for Hapstick to achieve the desired stiffness is obtained using results from Section III-B. This desired vacuum load is fed into the vacuum regulator as a digital signal, and the regulator then controls the vacuum load being drawn from Hapstick. Hapstick's stiffness varies depending on the level of vacuum being drawn, resulting in changes in its ability to resist motion. The user can perceive the stiffness of the environment through this resistance to motion, which is analogous to the resistance experienced by the teleoperated robot when interacting with the environment.

III. Device Characterization

The range of stiffnesses that Hapstick can achieve is dependent on its physical design parameters (i.e. diameter, fiber material, number of fibers, etc.) and the applied vacuum load. In this section, the effect of the number of fibers on Hapstick's mechanical behavior, specifically the force versus deflection behavior during bending, is presented. The results of the study help to inform the number of fibers required to provide uniform stiffness feedback to the users regardless of Hapstick configuration. In addition, the relationship between the applied vacuum and the resulting stiffness of the final Hapstick design is characterized in order to facilitate the design of controllers and haptic rendering algorithms. It should be noted that although fiber-jamming based structures have been shown to have motion hysteresis in their force versus deflection behavior [12], only loading (and not unloading) conditions are considered for the following experiments and characterization, based on previous studies [16] and [17]. These studies have shown that humans may detect stiffness during only the pushing motion, which corresponds to the loading of Hapstick.

A. Effects of Fiber Number

It has been shown that the fibers in fiber jamming-based structures, similar to Hapstick, experience slipping with respect to each other when subjected to large deflections. This phenomenon occurs because of the inability of the friction forces between the fibers to hold their relative motion [12]. Using cantilever loading, a force versus deflection curve can be generated and its slope can be measured to observe the slipping transition [10], [12]. After the slipping transition, the slope of this curve decreases, which causes the stiffness of the bent fiber jamming-based structure to significantly drop when deflected further [10]. It is also to be noted that when a fiber jamming-based structure is subjected to a smaller vacuum load, the slipping transition occurs at a smaller deflection [10].

For a given vacuum load, Hapstick would ideally be able to render uniform stiffness to the users regardless of its configuration, i.e. its state of deflection. The desired uniformity in rendered stiffness can be achieved by minimizing the effects of the slipping transition between the fibers for a large range of deflections, even at small vacuum loads. In [10], the FEA-based model that is presented to predict the force required for the slipping transition suggests that by sufficiently increasing the area moment of inertia of a fiber jamming structure, its slipping

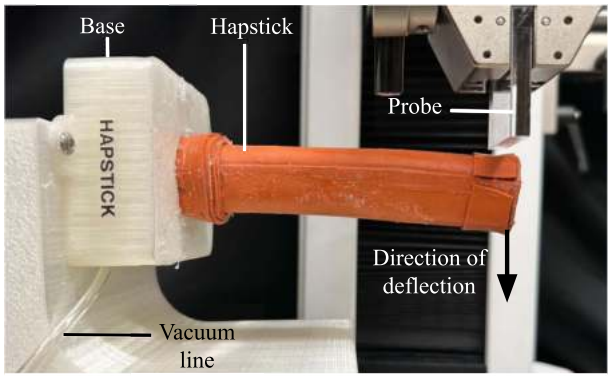

Fig. 4. Hapstick in a cantilever beam configuration for the characterization study of its force versus deflection behavior.

transitions can be avoided for large deflections. One way to increase the area moment of inertia of a fiber jamming-based structure of a given dimension is to increase the number of equally dimensioned fibers.

In this study, we perform an experiment to find the number of fibers required to obtain a linear force versus deflection curve, which signals minimal slipping, at least up to the studied maximum deflection. Five different amounts of fibers — namely 89, 139, 189, 239, and 289 fibers — were studied under two vacuum loads, 0 kPa and 70 kPa. The largest number of fibers used in the study represents the maximum possible number of fibers that could fit inside the soft silicone envelope. Similarly, 70 kPa was the largest vacuum load that could be obtained using the vacuum pump employed in this study. A Mark-10 tensile tester with an acrylic probe was used to deflect the tip of Hapstick, which was positioned in a cantilever beam configuration as seen in Fig. 4. Cantilever loading is a simple representation of the loading case that Hapstick is subjected to during its usage. Hapstick was deflected up to 40 mm, which is the largest deflection at which the probe consistently remained in contact with the Hapstick tip, at the rate of 2 mm/s. The forces and deflections measured using the tensile tester were recorded, and the corresponding force versus deflection curves, such as those in Fig. 5(a), were generated. Three trials were run for each fiber count at each vacuum load.

Fig. 5(b) shows the results of the average R^2 values observed in the generated force versus deflection plots. The force versus deflection curves for Hapsticks with the studied number of fibers were fairly linear when Hapsticks were subjected to large vacuum loads. However, for Hapsticks without any vacuum load, the linearity of the force versus deflection plots substantially improved with an increase in the number of fibers. At the largest studied number of fibers, the R^2 values for the force versus deflection plots at both 0 kPa and 70 kPa were ~ 0.99. Therefore, when the number of fibers in the designed Hapstick is maintained at 289, the slipping transition has negligible effects on Hapstick's stiffness for up to at least 40 mm of tip deflection for any vacuum load between 0 kPa and 70 kPa. We note that one downside of using a larger number of fibers is that the base stiffness of Hapstick (i.e the stiffness when the vacuum load is absent) is increased, meaning that the lowest stiffness value that can be rendered is also increased. Ultimately, we selected to use the maximum number of fibers in the final design to ensure that, for a given vacuum load, it can display uniform stiffness to the users regardless of its configuration.

B. Stiffness Characterization

After fabricating a Hapstick with 289 fibers, we performed an experiment using the same setup as that used in Section III-A to calculate the stiffness of the final Hapstick design when it is subjected to vacuum loads of 0 kPa to 70 kPa in step sizes of 7 kPa. The goal of the study was to characterize the physical stiffnesses that the fabricated Hapstick can acquire when different vacuum loads are applied. An established relationship between Hapstick stiffness and applied vacuum load can facilitate the design of appropriate haptic rendering algorithms and controllers. Three trials were run at each vacuum load, and the resulting stiffness values were calculated by measuring the slopes generated from the obtained force versus deflection plots. In order to respect the criteria of force acting perpendicularly at the tip of the cantilever beam during the measurements, deflections up to only 8.75 mm, which corresponds to the deflection angle of 5°,were considered during these stiffness calculations. The mean stiffness values and standard deviations are plotted in Fig. 5(c) for each vacuum load. A linear relationship is observed between the Hapstick stiffness (K_{H}) and the applied vacuum load (P) as given by:

$$K_{\mathrm{H}} = 2.20 \cdot P + 38.63. \quad (1)$$

Stiffnesses corresponding to any vacuum loads between 0 kPa and 70 kPa can be interpolated using the obtained relationship, given by (1). Based on these results, the Hapstick stiffness when no vacuum load is applied is 38.63 N/m and the stiffness measured at the vacuum load of 70 kPa is 192.63 N/m. Therefore, the maximum jamming ratio, defined as the stiffness at the maximum vacuum load divided by the stiffness when no vacuum load is applied, is 4.99.

IV. Psychophysical Study of Stiffness Perception

A psychophysical experiment was conducted to obtain the just noticeable difference (JND) in stiffness that users can perceive using Hapstick, given any reference stiffness. Measurements were obtained from users bending Hapstick in leftward and rightward directions to observe potential differences in user perception when using the device during pronation and supination of the wrist. This experimentally obtained JND for the chosen reference stimulus is used to compute the constant Weber Fraction (WF). According to Weber's Law, the WF is a constant ratio between the JND and a reference input stimulus [18]. The linear relationship given by the WF thus allows for estimating the JND for any reference stiffnesses displayed by Hapstick (i.e. $\mathrm{JND} = \mathrm{WF} \times K_{\mathrm{ref}}$).

A. Participants

Twelve participants aged 18–29 were recruited for the study (6 female and 6 male). Out of the twelve users, eleven were

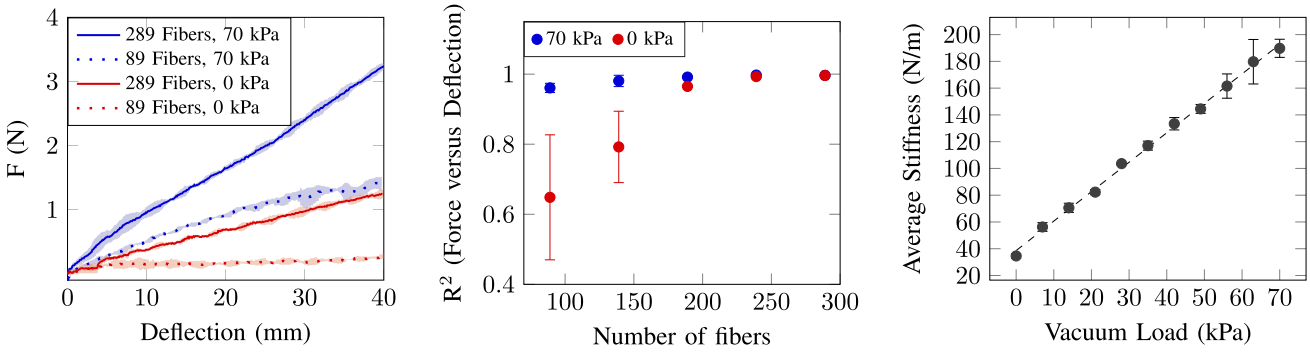

(a) (b) (c)

Fig. 5. (a) Force versus deflection plots with their standard deviations generated for Hapstick with the largest and the smallest studied number of fibers, 289 and 89 respectively, at a large vacuum load (70 kPa) and no vacuum load (0 kPa). For Hapstick with 289 fibers, the slopes of the obtained plots are consistent for tip deflections between 0 mm and 40 mm.(b) Average R^2 values calculated from the obtained force versus deflection plots for Hapsticks with different numbers of fibers at the vacuum loads of 70 kPa and 0 kPa. R^2 values generally increased with the increase in the number of fibers. (c) The obtained linear relationship between the applied vacuum load and average Hapstick stiffness for the final Hapstick design with 289 fibers.

right-hand-dominant, and five reported having had prior experience with haptic devices. All participants gave informed consent, and the experiment was approved by the University of California, San Diego, Institutional Review Board.

B. Methods

To obtain the JND at a reference stimulus, the method of constant stimuli was used, whereby a set of comparison stimuli are compared against a reference stimulus [19]. A two-alternative forced-choice (2AFC) procedure was used, where users responded yes or no to the question "was the second stiffness greater than the first stiffness?"

Before beginning the study, all participants were trained on how to interact with Hapstick. Users were instructed to grasp the device using a power grip and were asked to displace it left or right until it stiffened. Once the device stiffened, users were instructed to palpate the stiffened Hapstick within a 20 mm region, in order to simulate a tissue palpation task. All participants were given 2 minutes to familiarize themselves with the device. They then completed a training session that consisted of 14 trials that were conducted identically to those in the actual study, except that they were notified of the correct response after each training trial.

During each trial, participants stood in front of Hapstick and were provided with a sequence of instructions via the Arduino serial monitor. Users were required to center Hapstick for 3 seconds, then were instructed to bend the device either left or right. After bending Hapstick such that its tip was displaced more than 20 mm, a reference stiffness of 104.8 N/m (corresponding to 30 kPa applied vacuum load) was provided. Users were given 5 seconds to palpate the device in order to perceive its stiffness. After palpating, users were instructed to return Hapstick back to its center for 3 seconds. Subjects then repeated the above sequence but were instead given one of the following comparison stiffness values: 60.7, 82.7, 104.7, 126.8, 148.8, 170.9, or 192.9 N/m. The order and direction in which these comparison stimuli were provided were randomly pre-generated

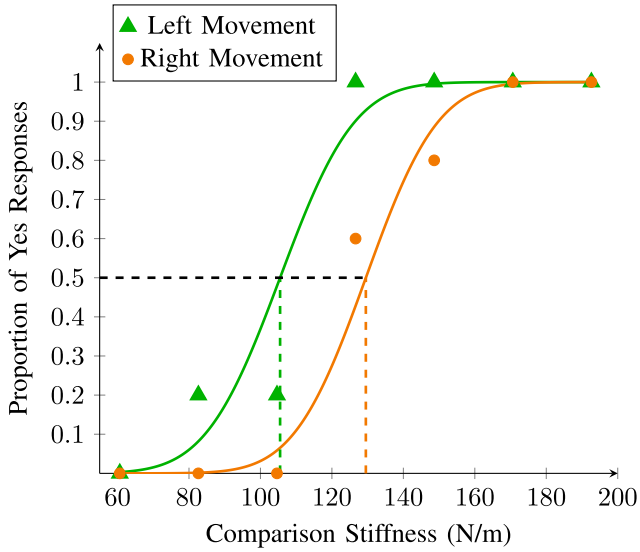

Fig. 6. Representative psychometric curves obtained for one participant for movement in both the left and right directions.

and presented to all users. All participants performed 70 total trials, 5 times per comparison stimulus in leftward and rightward directions. Users recorded their responses into the Arduino serial monitor by entering "y" to indicate that the second stimulus was stiffer than the first, or "n" otherwise. Additionally, participants wore active noise-canceling headphones playing white noise in order to prevent them from hearing any relative difference in noise generated by the vacuum regulator.

C. Results and Discussion

Representative psychometric curves are shown in Fig. 6 for leftward and rightward movement. These curves were generated using the Psignifit toolbox for MATLAB [20]. The toolbox plots the proportion of "yes" responses against the corresponding comparison stiffness values and fits a psychometric curve to the data points. The point of subjective equality (PSE) (i.e. the

TABLE I
SUMMARY OF RESULTS OBTAINED FROM THE PERFORMED PSYCHOPHYSICAL STUDY FOR A REFERENCE STIMULUS OF 104.63 N/M

	Left Movement			Right Movement		
Subject	PSE (N/m)	JND (N/m)	WF (%)	PSE (N/m)	JND (N/m)	WF (%)
1	105.6	49.7	47.1	129.7	49.4	38.1
2	120.4	70.8	58.9	136.4	77.5	56.8
3	134.6	70.7	52.5	119.8	72.9	60.9
4	114.7	50.5	44.0	90.3	47.3	52.4
5	143.5	95.1	66.3	95.0	79.7	83.9
6	120.6	46.8	38.8	93.7	46.2	49.3
7	129.0	59.6	46.2	103.7	49.7	47.9
8	96.4	64.5	66.9	91.4	63.4	69.4
9	159.0	69.0	43.4	116.9	51.8	44.3
Mean	124.9	64.1	51.6	108.5	59.8	55.9
STD	19.2	14.9	10.3	17.6	13.7	14.0

comparison value that over a large number of trials is perceived by users to be equivalent to the reference [19]), along with the 25th and 75th percentile comparison values, are obtained from the psychometric curve. The JND is computed using the PSE as well as the 25th and 75th percentile comparison values (P_{25} and P_{75}) as follows:

$$\text{JND} = \frac{(P_{75} - \text{PSE}) + (\text{PSE} - P_{25})}{2}. \tag{2}$$

The Weber Fraction is estimated using the empirically determined JND and PSE measures as follows:

$$\text{WF} = \frac{\text{JND}}{\text{PSE}}. \tag{3}$$

A summary of the experimental results is shown in Table I. An outlier detection test was used to identify anomalies in the psychometric data, which can often occur in psychophysical studies due to the study design or instruction, or due to participants becoming bored or fatigued [21]. The method used to identify these outliers was S_n [22], as it was shown to be suitable for detecting outliers in data obtained from psychometric experiments [21]. The method was performed on the PSE values because these measurements provide an indication of the constant error, or the error between what users perceive to be the reference stimulus and the true reference stimulus [19]. Out of the twelve initial users, three users were classified as outliers. Psychophysical studies relating to haptic perception tend to be lengthy [19], and it is suspected that the lengthy nature of this study caused these users to become fatigued or to become distracted.

Given a reference input stimulus of 104.75 N/m, the average JND was 64.1 N/m for leftward movement and 59.8 N/m for rightward movement. The Weber Fractions obtained for leftward and rightward movements were 51.6% and 55.9%, respectively. Although previous studies have shown that WFs related to stiffness discrimination typically range from 15–28% [23], [24], studies investigating the WF for the moment of inertia have shown significantly higher values, ranging from 10–113% [25] [26]. Given that the stimuli provided by Hapstick involve changes in both the stiffness and moment of inertia, the resulting WFs seem reasonable.

User responses were taken for movements in leftward and rightward bending directions to observe potential differences in stiffness perception. A Shapiro-Wilk test (5% significance level) was used to verify that the PSE measurements in both directions were normally distributed. A two-sample t-test (5% significance level) revealed that there was no statistical difference in PSE measurements for the leftward and rightward movement. This result implies that users are able to perceive the stiffnesses generated by Hapstick equivalently in both directions.

V. DEMONSTRATED TUMOR IDENTIFICATION TASK AND RESULTS

In this section, we demonstrate the ability of Hapstick to be used as a haptic interface for teleoperating a continuum robot and its ability to provide tunable stiffness feedback in multiple directions. We focus here on colorectal cancer screening, where the inside of the colon tissue is palpated to identify cancerous tissues, which are stiffer than their non-cancerous counterparts [27]. In particular, users are asked to identify three development stages of colon tumors, namely T2, T3, and T4, since their correct evaluation influences surgical and therapeutic approaches taken for treatment of colorectal cancer [28].

A. Setup

Users sit facing Hapstick and are asked to wear noise-canceling headphones. Their interactions with Hapstick are measured and mapped to the movements of a two-segment tendon-driven robot. κ_{H} is mapped to κ_{R} after being scaled by a factor of 0.2 and ϕ_{H} is mapped directly to ϕ_{R}, as described in Section II-C. The robot is centered inside an acrylic tube, designed to mimic a section of a colon. The colon model itself is lined with images of the colon wall, however, cancerous tissues cannot be visually identified. When the robot's tip position, computed using the forward-kinematics, coincides with the known position of the wall of the colon model, Hapstick's stiffness is changed based on the tissue to be rendered in that region. In the future, a probe with a force sensor, such as the one presented in [14], could be attached at the tip of the follower continuum robot for real-time tissue stiffness measurement. Finally, an Accfly Mini Pinhole 3.6 mm camera is mounted to the tip of the robot and is used to capture real-time video inside the colon model during the task. The setup consisting of the robot and colon model shown in Fig. 7(b) is hidden from the user, who can only view Hapstick, the button, and the video stream as shown in Fig. 7(a).

B. Procedure and Results

Three right-handed users, who were all previously trained to use Hapstick (either through pilot studies or the previously described JND study) were recruited for this demonstration. The participants were trained to identify the three studied tumor stages and to teleoperate the tendon-driven robot, whose tip motion could be observed via real-time video displayed on the computer screen. Regions representing T2, T3, and T4 tumors were randomly positioned, with the only constraints being that there should not be tumor regions directly adjacent to one another

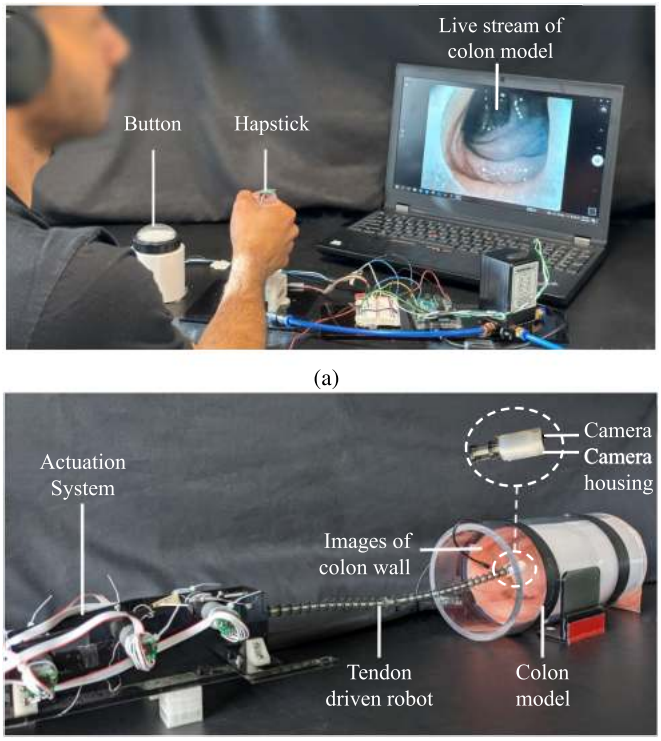

Fig. 7. (a) During a simulated colorectal cancer screening task, the surgeon-side interface consists of Hapstick and a screen for viewing real-time video streaming from a camera at the tip of the robot. (b) The patient-side setup consists of a tendon-driven continuum robot inside a colon model.

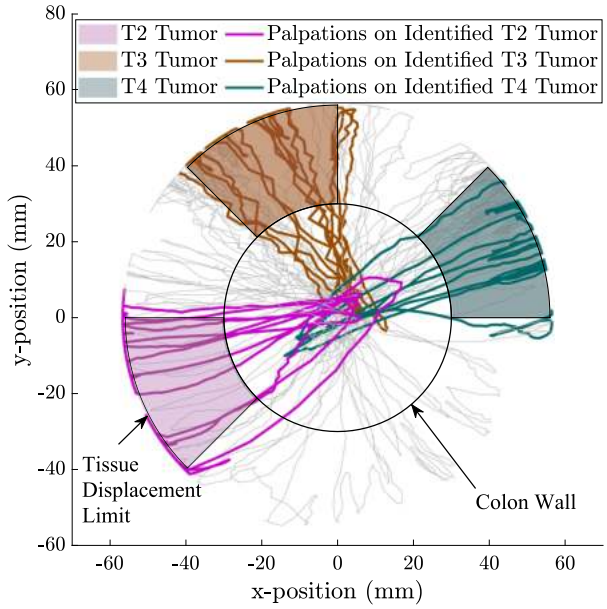

Fig. 8. A representative trajectory of the tendon-driven robot's tip over one trial. Gray lines indicate the trajectory of the robot's tip during exploratory palpations, and colored lines show the trajectory as the robot palpates on identified tumors, for the duration the button is pressed.

and each tumor should span a 45° interval, as shown in Fig. 8. The stiffnesses displayed by Hapstick for the cancerous tumors are selected such that they fall within the range of stiffnesses that can be displayed by the final Hapstick design, as described in Section III-B. These stiffness values are proportional to the median elastic moduli of the cancerous tumors at the given development stages, as presented in [27]. The stiffness values displayed by Hapstick for T2, T3, and T4 tumors are therefore 44 N/m, 113 N/m, and 177 N/m, respectively. For non-cancerous tissue regions, stiffness was not actively displayed, and users simply felt Hapstick's implicit stiffness of 38.63 N/m.

During the task, users were told to first palpate the tendon-driven robot clockwise around the circumference of the entire model. Users were then allowed to freely explore the environment to identity the tumor regions and the corresponding development stages. Once users were ready to report their responses, they were instructed to palpate clockwise around the colon model as before, and to press and hold a button in the regions where they encountered a tumor. As users entered into these regions, they were also instructed to verbally report whether they were feeling a T2, T3, or T4 tumor. It should be noted that the robot's tip could not actually move past the colon model's rigid wall, due to the physical constraint. However, the user could still use Hapstick to teleoperate a virtual representation of the robot tip up until the tissue displacement limit, shown in Fig. 8, to simulate pushing against a deformable tissue.

Three users performed three trials of the task. A representative trajectory of the tendon-driven robot's tip position over one trial is shown in Fig. 8. Participants were able to successfully identify the position and the development stage of the cancerous tumors with 92.6% accuracy (i.e 25 out of 27 responses were correct) using the stiffness feedback displayed by Hapstick. One user misidentified T3 as T4, and vice versa. This can be attributed to the JND being larger for larger stiffnesses corresponding to T3 and T4 tumors, as determined by the WF. Despite the small difference in stiffnesses between T2 tumors and non-cancerous tissue, T2 tumors were correctly identified in all trials. The cutaneous feedback resulting from deformation of the soft envelope, along with kinesthetic feedback, could have potentially aided this distinction.

VI. Conclusion

In this letter, we proposed and characterized Hapstick, a flexible input device that can provide tunable stiffness feedback via fiber jamming. We found that by increasing the number of fibers, Hapstick could display a more uniform stiffness feedback even at small vacuum loads and large deflections. Hapstick's final design exhibited a linear relationship between the achieved stiffnesses and the applied vacuum loads. The final Hapstick design can acquire any stiffness between 38.63 N/m and 192.63 N/m. Users' ability to perceive the stiffnesses that can be displayed by Hapstick was also characterized in the Just Noticeable Difference (JND) study. The average Weber Fraction (WF) was found to be 51.9% $\pm$ 10.3% during the leftward movement and 55.9% $\pm$ 14.0% during the rightward movement. JND at any reference stimulus can be calculated using the obtained WF. Finally, the applicability of Hapstick for teleoperating a tendon-driven robot for colorectal cancer screening was demonstrated. Users

could correctly identify the cancerous regions along with their development stages with 92.6% accuracy.

As a continuation of this work, improvements in the device design, along with extensions to the performed studies, can be completed to further enhance Hapstick's capabilities. For example, given that the abrasive coating on the fibers can wear off after repeated usage, the device durability can be characterized and possibly improved. Future work can include the investigation of alternative fibers that enable fiber jamming-based devices to attain large stiffnesses even after repeated usage. Similarly, Hapstick's design can be refined to be more ergonomic in order to enable ease of motion regardless of the bending direction. As an extension of the performed psychophysical study, the JND can also be characterized for directions other than the already studied left and right directions. Finally, future studies can investigate the effectiveness of novel mapping techniques for teleoperating other types of continuum robots for a range of applications. Overall, Hapstick has illustrated the potential of jamming-based mechanisms as bidirectional interfaces capable of providing effective haptic feedback.

REFERENCES

[1] G. Robinson and J. B. C. Davies, "Continuum robots-a state of the art," in *Proc. IEEE Int. Conf. Robot. Automat.*, 1999, vol. 4, pp. 2849–2854.

[2] J. Burgner-Kahrs, D. C. Rucker, and H. Choset, "Continuum robots for medical applications: A survey," *IEEE Trans. Robot.*, vol. 31, no. 6, pp. 1261–1280, Dec. 2015.

[3] R. Scott, A. Kapadia, and I. Walker, "Intuitive interfaces for teleoperation of continuum robots," in *Proc. Int. Conf. Appl. Hum. Factors Ergonom.*, 2018, pp. 77–89.

[4] R. J. Webster III and B. A. Jones, "Design and kinematic modeling of constant curvature continuum robots: A review," *Int. J. Robot. Res.*, vol. 29, no. 13, pp. 1661–1683, 2010.

[5] H.-S. Yoon and B.-J. Yi, "Design of a master device for controlling multi-moduled continuum robots," *Proc. Inst. Mech. Eng., Part C: J. Mech. Eng. Sci.*, vol. 231, no. 10, pp. 1921–1931, 2017.

[6] H. El-Hussieny et al., "Development and evaluation of an intuitive flexible interface for teleoperating soft growing robots," in *Proc. IEEE/RSJ Int. Conf. Intell. Robots Syst.*, 2018, pp. 4995–5002.

[7] C. G. Frazelle, A. D. Kapadia, and I. D. Walker, "A haptic continuum interface for the teleoperation of extensible continuum manipulators," *IEEE Robot. Automat. Lett.*, vol. 5, no. 2, pp. 1875–1882, Apr. 2020.

[8] M. Manti, V. Cacucciolo, and M. Cianchetti, "Stiffening in soft robotics: A review of the state of the art," *IEEE Robot. Automat. Mag.*, vol. 23, no. 3, pp. 93–106, Sep. 2016.

[9] I. Zubrycki and G. Granosik, "Novel haptic glove-based interface using jamming principle," in *Proc. 10th Int. Workshop Robot Motion Control*, 2015, pp. 46–51.

[10] S. Jadhav, M. R. A. Majit, B. Shih, J. P. Schulze, and M. T. Tolley, "Variable stiffness devices using fiber jamming for application in soft robotics and wearable haptics," *Soft Robot.*, vol. 9, no. 1, pp. 173–186, 2022.

[11] I. Zubrycki and G. Granosik, "Novel haptic device using jamming principle for providing kinaesthetic feedback in glove-based control interface," *J. Intell. Robot. Syst.*, vol. 85, no. 3, pp. 413–429, 2017.

[12] M. Brancadoro, M. Manti, S. Tognarelli, and M. Cianchetti, "Fiber jamming transition as a stiffening mechanism for soft robotics," *Soft Robot.*, vol. 7, no. 6, pp. 663–674, 2020.

[13] G. Harih and B. Dolšak, "Comparison of subjective comfort ratings between anatomically shaped and cylindrical handles," *Appl. Ergonom.*, vol. 45, no. 4, pp. 943–954, 2014.

[14] T. Nagatomo and N. Miki, "Three-axis capacitive force sensor with liquid metal electrodes for endoscopic palpation," *Micro Nano Lett.*, vol. 12, no. 8, pp. 564–568, 2017.

[15] K. Salisbury, D. Brock, T. Massie, N. Swarup, and C. Zilles, "Haptic rendering: Programming touch interaction with virtual objects," in *Proc. Symp. Interactive 3D Graph.*, 1995, pp. 123–130.

[16] A. Pressman, L. J. Welty, A. Karniel, and F. A. Mussa-Ivaldi, "Perception of delayed stiffness," *Int. J. Robot. Res.*, vol. 26, no. 11–12, pp. 1191–1203, 2007.

[17] N. Gurari, K. J. Kuchenbecker, and A. M. Okamura, "Perception of springs with visual and proprioceptive motion cues: Implications for prosthetics," *IEEE Trans. Human-Mach. Syst.*, vol. 43, no. 1, pp. 102–114, Jan. 2012.

[18] G. A. Gescheider, *Psychophysics: The Fundamentals*. London, U.K.: Psychology Press, 2013.

[19] L. A. Jones and H. Z. Tan, "Application of psychophysical techniques to haptic research," *IEEE Trans. haptics*, vol. 6, no. 3, pp. 268–284, Jul.–Sep. 2013.

[20] I. Fründ, N. V. Haenel, and F. A. Wichmann, "Inference for psychometric functions in the presence of nonstationary behavior," *J. Vis.*, vol. 11, no. 6, pp. 16–16, 2011. [Online]. Available: http://www.journalofvision.org/content/11/6/16

[21] P. R. Jones, "A note on detecting statistical outliers in psychophysical data," *Attention, Percep., Psychophys.*, vol. 81, no. 5, pp. 1189–1196, 2019.

[22] P. J. Rousseeuw and C. Croux, "Alternatives to the median absolute deviation," *J. Amer. Stat. Assoc.*, vol. 88, no. 424, pp. 1273–1283, 1993.

[23] W. M. B. Tiest and A. M. Kappers, "Cues for haptic perception of compliance," *IEEE Trans. haptics*, vol. 2, no. 4, pp. 189–199, Oct.–Dec. 2009.

[24] L. A. Jones and I. W. Hunter, "A perceptual analysis of stiffness," *Exp. Brain Res.*, vol. 79, no. 1, pp. 150–156, 1990.

[25] J. G. Kreifeldt and M.-C. Chuang, "Moment of inertia: Psychophysical study of an overlooked sensation," *Science*, vol. 206, no. 4418, pp. 588–590, 1979.

[26] H. Ross and A. Benson, "The Weber fraction for moment of inertia," *Fechner Day*, vol. 86, pp. 71–76, 1986.

[27] S. Kawano et al., "Assessment of elasticity of colorectal cancer tissue, clinical utility, pathological and phenotypical relevance," *Cancer Sci.*, vol. 106, no. 9, pp. 1232–1239, 2015.

[28] P. P. Mainenti et al., "Colorectal cancer and 18fdg-pet/ct: What about adding the t to the n parameter in loco-regional staging," *World J. Gastroenterol.: WJG*, vol. 17, no. 11, pp. 1427–1433, 2011.